

# MultiBooth: Towards Generating All Your Concepts in an Image from Text

Chenyang Zhu<sup>1</sup>, Kai Li<sup>2†</sup>, Yue Ma<sup>1</sup>, Chunming He<sup>1</sup>, and Xiu Li<sup>1†</sup>

<sup>1</sup> Tsinghua University, SIGS

<sup>2</sup> Meta Reality Labs

<https://multibooth.github.io/>



**Fig. 1: MultiBooth** can learn individual customization concepts through a few examples and then combine these learned concepts to create multi-concept images based on text prompts. The results indicate that our MultiBooth can effectively preserve high image fidelity and text alignment when encountering complex multi-concept generation demands, including (a) restylization, (b) different spatial relationships, and (c) recontextualization.

**Abstract.** This paper introduces MultiBooth, a novel and efficient technique for multi-concept customization in image generation from text. Despite the significant advancements in customized generation methods, particularly with the success of diffusion models, existing methods often struggle with multi-concept scenarios due to low concept fidelity and high inference cost. MultiBooth addresses these issues by dividing the multi-concept generation process into two phases: a single-concept learning phase and a multi-concept integration phase. During the single-concept learning phase, we employ a multi-modal image encoder and an efficient concept encoding technique to learn a concise and discriminative representation for each concept. In the multi-concept integration phase, we use bounding boxes to define the generation area for each concept within the cross-attention map. This method enables the creation of individual

† Corresponding authors.

concepts within their specified regions, thereby facilitating the formation of multi-concept images. This strategy not only improves concept fidelity but also reduces additional inference cost. MultiBooth surpasses various baselines in both qualitative and quantitative evaluations, showcasing its superior performance and computational efficiency.

**Keywords:** Text-to-image generation · personalized image generation · multi-concept customization

## 1 Introduction

The advent of diffusion models has ignited a new wave in the text-to-image (T2I) task, leading to the proposal of numerous models [4, 5, 9, 13, 17, 23, 28, 31, 34]. Despite the broad capabilities of these models, users often desire to generate specific concepts such as beloved pets or personal items. These personal concepts are not captured during the training of large-scale T2I models due to their subjective nature, emphasizing the need for customized generation [1, 2, 8, 10, 14–16, 24, 29]. Customized generation aims to create new variations of a given concept, including different contexts (e.g., beaches, forests) and styles (e.g., painting), based on just a few user-provided images (typically fewer than 5).

Recent customized generation methods either learn a concise token representation for each subject [17] or adopt an efficient fine-tuning strategy to adapt the T2I model specifically for the subject [24]. While these methods have achieved impressive results, they primarily focus on single-concept customization and struggle when users want to generate customized images for multiple subjects (see Fig. 2). This motivates the study of multi-concept customization (MCC).

Existing methods [8] for MCC commonly employ joint training approaches. However, this strategy often leads to feature confusion, as illustrated in the third column of Fig. 2. Furthermore, these methods require training distinct models for each combination of subjects and are hard to scale up as the number of subjects grows. An alternative method [10] addresses MCC by adjusting attention maps with residual token embeddings during inference. While this approach shows promise, it incurs a notable inference cost. Furthermore, the method encounters difficulties in attaining high fidelity due to the restricted learning capacity of a single residual embedding.

To address the aforementioned issues, we introduce MultiBooth, a two-phase MCC solution that accurately and efficiently generates customized multi-concept images based on user demand, as demonstrated in the Fig. 2. MultiBooth includes a discriminative single-concept learning phase and a plug-and-play multi-concept integration phase. In the former phase, we learn each concept separately, resulting in a single-concept module for every concept. In the latter phase, we effectively combine these single-concept modules to generate multi-concept images without any extra training.

More concretely, we propose the Adaptive Concept Normalization (ACN) to enhance the representative capability of the generated customized embedding in the single-concept learning phase. We employ a trainable multi-model encoder

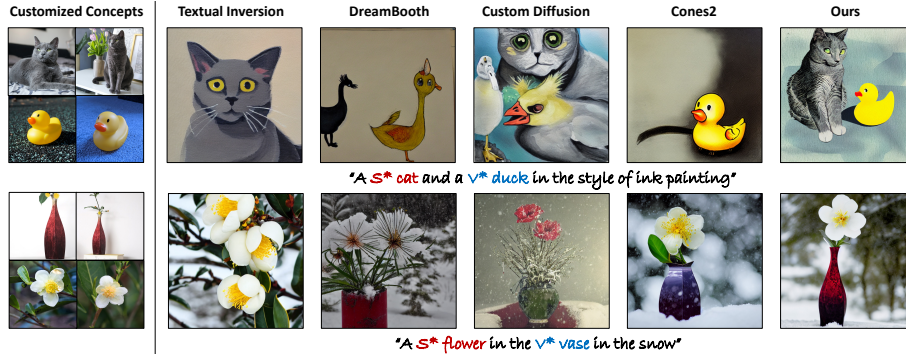


**Fig. 2: Results of single-concept methods (Text-Inversion [1] and DreamBooth [24]) and multi-concept methods (Custom Diffusion [8], Cone2 [10], and our MultiBooth).** Traditional single-concept methods are inadequate when it comes to accommodating multi-concept customization, whereas existing multi-concept approaches often struggle with maintaining high fidelity and prompt alignment.

to generate customized embeddings, followed by the ACN to adjust the L2 norm of these embeddings. Finally, by incorporating an efficient concept encoding technique, all detailed information of a new concept is extracted and stored in a single-concept module which contains a customized embedding and the efficient concept encoding parameters.

In the plug-and-play multi-concept integration phase, we further propose a regional customization module to guide the inference process, allowing the correct combination of different single-concept modules for multi-concept image generation. Specifically, we divide the attention map into different regions within the cross-attention layers of the U-Net, and each region’s attention value is guided by the corresponding single-concept module and prompt. Through the proposed regional customization module, we can generate multi-concept images via any combination of single-concept modules while bringing minimal cost during inference.

Our approach is extensively validated with various representative subjects, including pets, objects, scenes, etc. The results from both qualitative and quantitative comparisons highlight the advantages of our approach in terms of concept fidelity and prompt alignment capability. Our contributions are summarized as follows:

- We propose a novel framework named MultiBooth. It allows plug-and-play multi-concept generation after separate customization of each concept.
- The adaptive concept normalization is proposed in our MultiBooth to mitigate the problem of domain gap in the embedding space, thus learning a representative customized embedding. We also introduce the regional customization module to effectively combine multiple single-concept modules for multi-concept generation.
- Our method consistently outperforms current methods in terms of image quality, faithfulness to the intended concepts, and alignment with the text prompts.

## 2 Related Work

### 2.1 Text to Image Generation

Text-to-image generation is an extensively researched problem, with numerous early studies focusing on Generative Adversarial Networks (GANs) [3]. Noteworthy examples include AttnGAN [30], StackGAN [32], StackGAN++ [33], Mirrorgan [20]. While these methods have proven to be effective on specific datasets such as faces and landscapes, they have limited generalization ability to larger-scale datasets. Moreover, training GANs poses instability issues and is susceptible to mode collapse. With the advancements of diffusion models [6], more and more methods have started exploring text-to-image generation based on diffusion models. By training on large-scale text-image datasets such as LAION [26], these methods have achieved superior performance. Notable recent works include DALLE2 [22], Imagen [25], GLIDE [18], and Stable Diffusion [23], which are capable of generating images based on open-vocabulary text prompts.

### 2.2 Customized Text to Image Generation

The goal of customized text-to-image generation is to acquire knowledge of a novel concept from a limited set of examples and subsequently generate images of these concepts in diverse scenarios based on text prompts. By leveraging the aforementioned diffusion-based methodologies, it becomes possible to employ the comprehensive text-image prior to customizing the text-to-image process.

Textual Inversion [1] achieves customization by creating a new embedding in the tokenizer and associating all the details of the newly introduced concept to this embedding. DreamBooth [24] binds the new concept to a rare token followed by a class noun. This process is achieved by finetuning the entire diffusion model. Additionally, DreamBooth addresses the issue of language drift through a prior preservation loss. ELITE [29] utilizes multi-layer embeddings from CLIP image encoder [21] and employs a mapping network to acquire customized embeddings. Similar approaches are adopted in InstantBooth [27] and E4T [2]. Such encoder-based methods require less training time and yield better image generation results compared to directly optimizing the embedding in Textual Inversion [1]. Custom Diffusion [8] links a novel concept to a rare token by adjusting specific parameters of the diffusion model. To alleviate overfitting, Custom Diffusion also incorporates a regularization dataset. Through joint training, Custom Diffusion explores the problem of multi-concept customization for the first time. Cones2 [10] learns new concepts by adding a residual embedding on top of the base embedding and generates multi-concept images through attention map manipulation.

In this work, we utilize a multi-modal model and LoRA to discriminatively and concisely encode every single concept. Then, we introduce the regional customization module to efficiently and accurately produce multi-concept images.



### 3 Method

Given a series of images  $\mathcal{S} = \{X_s\}_{s=1}^S$  that represent  $S$  concepts of interest, where  $\{X_s\} = \{x_i\}_{i=1}^M$  denotes the  $M$  images belonging to the concept  $s$  which is usually very small (e.g.,  $M \leq 5$ ), the goal of multi-concept customization (MCC) is to generate images that include any number of concepts from  $\mathcal{S}$  in various styles, contexts, layout relationship as specified by given text prompts. MCC poses significant challenges for two primary reasons. Firstly, learning a concept with a limited number of images is inherently difficult. Secondly, generating multiple concepts *simultaneously and coherently* within the same image while faithfully adhering to the provided text is even harder.

To tackle these challenges, Custom Diffusion [8] simultaneously finetunes the model with all subjects of interest. This approach can lead to issues like feature confusion and inaccurate attribution (e.g., attributing dog features to a cat). For Cone2 [10], the process requires repetitive strengthening and weakening of the same concept features during the inference phase, which can result in a significant decrease in fidelity. To avoid these problems, we propose a method called MultiBooth. Our MultiBooth initially performs high-fidelity learning of a single concept. We employ a multi-modal encoder and the adaptive concept normalization strategy to obtain text-aligned representative customized embeddings. Additionally, the efficient concept encoding technique is employed to further improve the fidelity of single-concept learning. To generate multi-concept images, we employ the regional customization module. This module serves as a guide for multiple single-concept modules and utilizes bounding boxes to indicate the positions of each generated concept.

#### 3.1 Preliminaries

In this paper, the foundational model utilized for text-to-image generation is Stable Diffusion [23]. It takes a text prompt  $P$  as input and generates the corresponding image  $x$ . Stable diffusion [23] consists of three main components: an autoencoder ( $\mathcal{E}(\cdot), \mathcal{D}(\cdot)$ ), a CLIP text encoder  $\tau_\theta(\cdot)$  and a U-Net  $\epsilon_\theta(\cdot)$ . Typically, it is trained with the guidance of the following reconstruction loss:

$$\mathcal{L}_{rec} = \mathbb{E}_{z, \epsilon \sim \mathcal{N}(0,1), t, P} [\|\epsilon - \epsilon_\theta(z_t, t, \tau_\theta(P))\|_2^2], \quad (1)$$

where  $\epsilon \sim \mathcal{N}(0, 1)$  is a randomly sampled noise,  $t$  denotes the time step. The calculation of  $z_t$  is given by  $z_t = \alpha_t z + \sigma_t \epsilon$ , where the coefficients  $\alpha_t$  and  $\sigma_t$  are provided by the noise scheduler.

Given  $M$  images  $\{X_s\} = \{x_i\}_{i=1}^M$  of a certain concept  $s$ , previous works [1, 8, 24] associate a unique placeholder string  $S^*$  with concept  $s$  through a specific prompt  $P_s$  like “a photo of a  $S^*$  dog”, with the following finetuning objective:

$$\mathcal{L}_{bind} = \mathbb{E}_{z=\mathcal{E}(x), x \sim X_s, \epsilon, t, P_s} [\|\epsilon - \epsilon_\theta(z_t, t, \tau_\theta(P_s))\|_2^2]. \quad (2)$$

The result of minimizing Eq. (2) is to encourage the U-Net  $\epsilon_\theta(\cdot)$  to accurately reconstruct the images of the concept  $s$ , effectively binding the placeholder string  $S^*$  to the concept  $s$ .

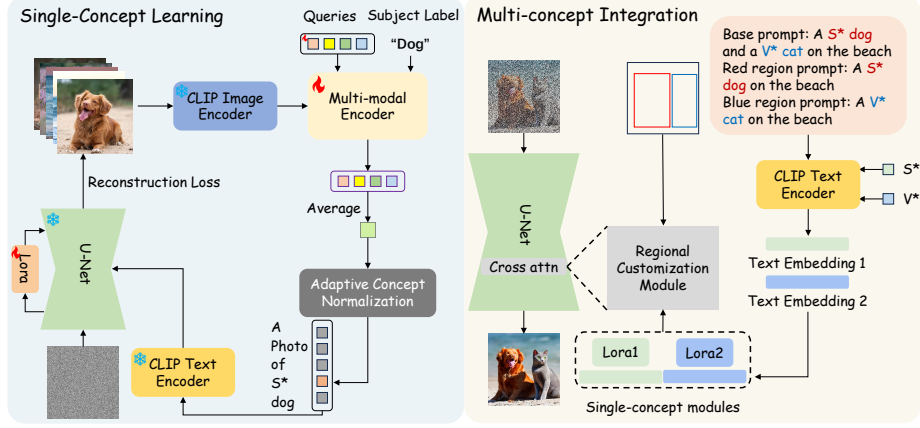


**Fig. 3: Overall Pipeline of MultiBooth.** (a) During the single-concept learning phase, a multi-modal encoder and LoRA parameters are trained to encode every single concept. (b) During the multi-concept integration phase, the customized embeddings  $S^*$  and  $V^*$  are converted into text embeddings, which are then combined with the corresponding LoRA parameters to form single-concept modules. These single-concept modules, along with the bounding boxes, are intended to serve as input for the regional customization module.

### 3.2 Single-Concept Learning

**Multi-modal Concept Extraction.** Existing methods [2, 29] mainly utilize a single image encoder to encode the concepts of interest. However, this approach may also encode irrelevant information, such as unrelated objects in the images. To remedy this, we employ a multi-modal encoder that takes as input both the images and the subject name (e.g., “dog”) to learn a concise and discriminative representation for each concept. Inspired by MiniGPT4 [35] and BLIP-Diffusion [9], we utilize the QFormer, a light-weighted multi-modal encoder, to generate customized concept embeddings. The QFormer encoder  $E$  has three types of inputs: visual embeddings  $\xi$  of an image, text description  $l$ , and learnable query tokens  $W = [w_1, \dots, w_K]$  where  $K$  is the number of query tokens. The outputs of QFormer are tokens  $O = [o_1, \dots, o_K]$  with the same dimensions as the input query tokens.

As shown in Fig. 3, given an image  $x_i \in X_s$ , we employ a frozen CLIP [21] image encoder to extract the visual embeddings  $\xi$  of the image. Subsequently, we set the input text  $l$  as the subject name for the image and input it into the encoder  $E$ . The learnable query tokens  $W$  interact with the text description  $l$  through a self-attention layer and with the visual embedding  $\xi$  through a cross-attention layer, resulting in text-image aligned output tokens  $O = E(\xi, l, W)$ . Finally, we obtain the initial customized embedding  $v_i$  by taking the average of these tokens:

$$v_i = \frac{1}{K} \cdot \sum_{i=1}^K o_i \quad (3)$$

**Table 1: Quantization results of the L2 norm of each word embedding in the prompt.** The customized embeddings of Textual Inversion and Ours w/o ACN have significantly larger L2 norm compared to other word embeddings in the prompt.

Method	a	S*	dog	and	a	V*	cat	on	the	beach
Textual Inversion [1]	0.35	<b>2.85</b>	-	0.34	0.35	<b>0.94</b>	-	0.34	0.34	0.37
Ours w/o ACN	0.35	<b>2.35</b>	0.37	0.34	0.35	<b>3.14</b>	0.37	0.34	0.34	0.37
Ours	0.35	<b>0.37</b>	0.37	0.34	0.35	<b>0.37</b>	0.37	0.34	0.34	0.37

where  $v_i \in \mathbb{R}^d$ ,  $d$  is the dimension of our customized embedding. Following [1, 8, 24], a placeholder string  $S^*$  is introduced to represent the newly acquired concept, with  $v_i$  representing its word embedding. Through this placeholder string  $S^*$ , we can easily activate the customized word embedding  $v_i$  to reconstruct the input concept image  $x_i$  with prompts like “a photo of a  $S^*$  dog”.

**Adaptive Concept Normalization** During the reconstruction with the prompt mentioned above, we have observed a domain gap between our customized embedding  $v_i$  and other word embeddings in the prompt. As shown in Tab. 1, the L2 norm of our customized embedding is considerably larger than that of other word embeddings in the prompt. Notably, these word embeddings, belonging to the same order of magnitude, are predefined within the embedding space of the CLIP text encoder  $\tau_\theta(\cdot)$ . This significant difference in quantity weakens the model’s ability for multi-concept generation. To remedy this, we further apply the Adaptive Concept Normalization (ACN) strategy to the customized embedding  $v_i$ , adjusting its L2 norm to obtain the final customized embedding  $\hat{v}_i$ .

The adaptive concept normalization strategy consists of two steps. The first step is L2 normalization, adjusting the L2 norm of the customized embedding  $v_i$  to 1. The second step is adaptive scaling, which brings the L2 norm of  $v_i$  to a comparable magnitude as other word embeddings in the prompt. Specifically, let  $c_l \in \mathbb{R}^d$  represent the word embedding corresponding to the subject name of  $v_i$  (e.g., the word embedding of “dog”), where  $d$  is the dimension of embeddings. The adaptive concept normalization can be expressed as:

$$\hat{v}_i = v_i \cdot \frac{\|c_l\|_2}{\|v_i\|_2} \quad (4)$$

where  $\hat{v}_i \in \mathbb{R}^d$  has the same dimensions as  $v_i$ . As shown in Tab. 1, this operation effectively addresses the problem of domain gap in the embedding space.

**Efficient Concept Encoding** Given the modified customized embedding  $\hat{v}_i$ , we can easily reconstruct the input image  $x_i$  through the text prompt  $P_s$  containing the placeholder string  $S^*$  (e.g., “a photo of a  $S^*$  dog”). To further improve the reconstruction fidelity during single-concept learning and avoid language drift caused by finetuning the U-Net, we incorporate the LoRA technique [7] for efficient concept encoding. Specifically, we incorporate a low-rank decomposition to the key and value weight matrices of attention layers within the U-Net  $e_\theta(\cdot)$ . Each pre-trained weight matrix  $W_{init} \in \mathbb{R}^{d \times k}$  is utilized in the forward

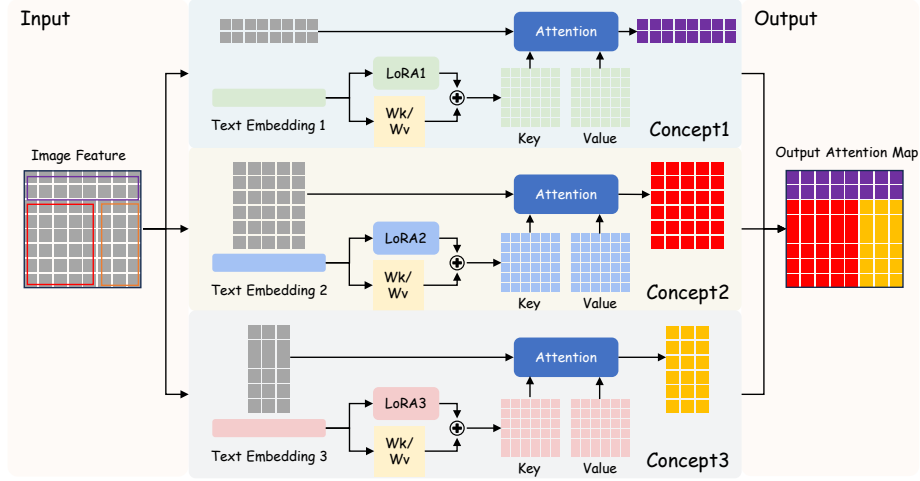


**Fig. 4: Regional Customization Module.** To generate individual concepts within their specified regions, we initially divide the image feature into several regions via bounding boxes to acquire the query  $Q$  for each concept. Subsequently, we combine the single-concept module with  $W_k$  and  $W_v$  to derive the corresponding key  $K$  and value  $V$ . After that, we perform the attention operation on the obtained  $Q$ ,  $K$ , and  $V$  to get a part of the final output. The above procedure is applied to each concept simultaneously, forming the final output attention map.

computation as follows:

$$h = W_{init}x + \Delta Wx = W_{init}x + BAx \quad (5)$$

where  $A \in \mathbb{R}^{r \times k}$ ,  $B \in \mathbb{R}^{d \times r}$  are trainable parameters of efficient concept encoding, and the rank  $r \ll \min(d, k)$ . During training, the pre-trained weight matrix  $W_{init}$  stays constant without receiving gradient updates.

The whole single-concept learning framework can be trained by optimizing Eq. (2) with a regularization term, as shown in the following equation:

$$\mathcal{L} = \mathbb{E}_{z=\mathcal{E}(x), x \sim \mathcal{X}_s, \epsilon, t, P_s} [\|\epsilon - \epsilon_\theta(z_t, t, \tau_\theta(P_s))\|_2^2] + \lambda \|\hat{v}_i\|_2^2 \quad (6)$$

where  $\lambda$  denotes a balancing hyperparameter and is consistently set to 0.01 across all experiments. During training, we randomly select text prompts  $P_s$  from the CLIP ImageNet templates [21] following the Textual Inversion [1]. The complete templates can be found in the *Suppl.* Through the above methods, the detailed information of a new concept can be extracted and stored in a customized embedding and corresponding LoRA parameters, which can be called a single-concept module. The storage requirement of a concept is less than 7MB, which is significantly advantageous compared to 3.3GB in [24] and 72MB in Custom Diffusion [8].

### 3.3 Multi-Concept Integration

**Regional Customization Module.** Our key insight is to restrict the generation of each concept within a given region. As illustrated in the right part of

Fig. 3, we propose the regional customization module in cross-attention layers, which makes it possible to integrate multiple LoRAs for multi-concept generation. Given a series of images  $\mathcal{S} = \{X_s\}_{s=1}^S$  that represent  $S$  concepts of interest, users can define the corresponding bounding boxes  $B = \{b_i\}_{i=1}^S$  and region prompts  $P_r = \{p_i\}_{i=1}^S$  for each concept, along with a base prompt  $p_{base}$ . The text embeddings  $C = \{c_i\}_{i=1}^S$  of each concept can be acquired using the CLIP text encoder, calculated as follows:

$$c_i = \tau_\theta(p_i) + \tau_\theta(p_{base}), i = 1, 2, \dots, S \quad (7)$$

where  $c_i \in \mathbb{R}^{k \times d}$  and  $k$  is the the maximum length of input words. Then, we perform the following operations on each concept simultaneously. As shown in Fig. 4, the image feature  $F \in \mathbb{R}^{(h \times w) \times l}$  is cropped using the bounding box  $b_i \in \mathbb{R}^{h_i \times w_i}$  of the  $i^{th}$  concept, resulting in the partial image feature  $f_i \in \mathbb{R}^{h_i \times w_i}$ . Subsequently, the query vector  $Q_i = W^q \cdot f_i$  is obtained. For the text embedding  $c_i$  and a set of LoRA parameters  $\{A_{ij}, B_{ij}\}_{i=1}^S$ , where  $A_{ij} \in \mathbb{R}^{r \times k}$  and  $B_{ij} \in \mathbb{R}^{d \times r}$ , with  $j = 1$  indicating the low-rank decomposition of  $W_k$  and  $j = 2$  indicating the low-rank decomposition of  $W_v$ , we can derive the key and value vector from:

$$K_i = W_k \cdot c_i + B_{i1}A_{i1} \cdot c_i \quad (8)$$

$$V_i = W_v \cdot c_i + B_{i2}A_{i2} \cdot c_i \quad (9)$$

The attention operation is then applied to the query, key, and value vectors to derive the image feature as follows:

$$\text{Attn}(Q_i, K_i, V_i) = \text{Softmax}\left(\frac{Q_i K_i^T}{\sqrt{d'}}\right) V_i \quad (10)$$

where  $W_q$ ,  $W_k$ , and  $W_v$  serve as projection matrices for the query, key, and value inputs, respectively, and  $d'$  represents the output dimension of key and query features. The obtained image feature  $\hat{f}_i = \text{Attn}(Q_i, K_i, V_i) \in \mathbb{R}^{h_i \times w_i}$  retains its original dimensions. The final output is calculated as  $\hat{F}[b_i] = \hat{f}_i$ , where any overlapping regions have their related features  $\hat{f}_i$  averaged.

The benefit of the proposed regional customization module is that each given region only interacts with the specific concept’s content during the cross-attention operation. This avoids the issue of mixing multi-concept features during cross-attention and allows each single-concept module to generate specific concepts following different text prompts in their respective regions. Moreover, the regional customization module brings minimal cost during inference, as evidenced in Tab. 2.

## 4 Experiment

### 4.1 Experimental Settings

**Implementation Details.** All of our experiments are based on Stable Diffusion [23] v1.5 and are conducted on a single RTX3090. We set the rank of LoRA to

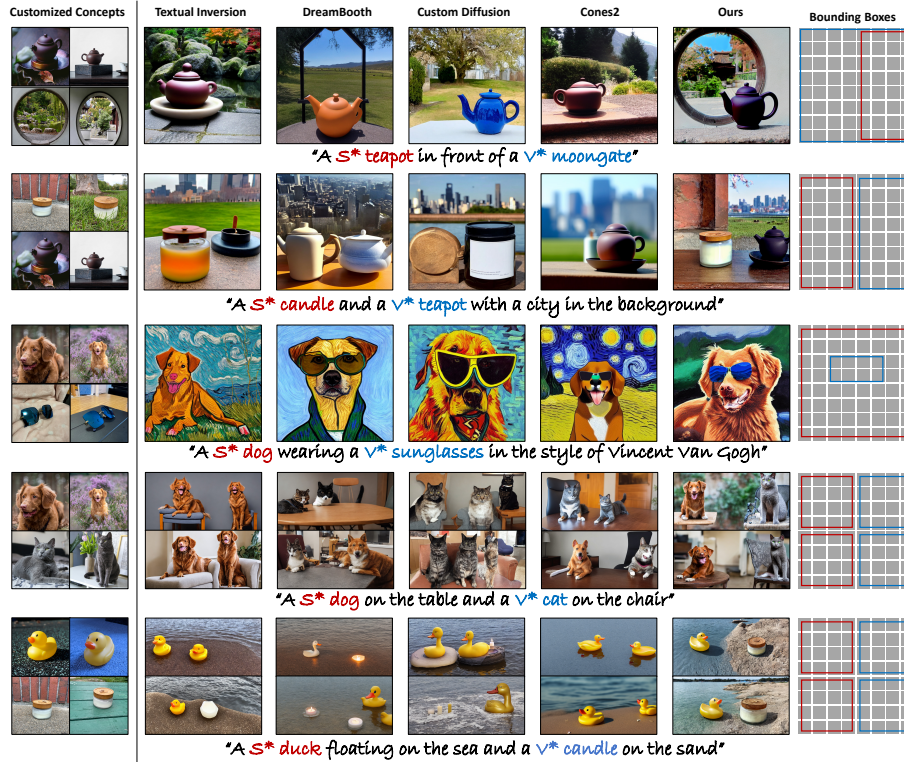


**Fig. 5: Qualitative comparisons.** Our method outperforms all the compared methods significantly in terms of image fidelity and prompt alignment capability.

be 16. We use the AdamW [11] optimizer with a learning rate of  $8 \times 10^{-5}$  and a batch size of 1, optimizing for 900 steps. During the inference stage, we utilize the DPM-Solver [12] for sampling 100 steps, with the guidance scale  $\omega = 7.5$ .


**Datasets.** Following Custom Diffusion [8], we conduct experiments on twelve subjects selected from the DreamBooth dataset [24] and CustomConcept101 [8]. They cover a wide range of categories including two scene categories, two pets, and eight objects.

**Evaluation Metrics.** As shown in Fig. 6, we have observed that when redundant elements dominate the calculation of the CLIP image score, it can result in high CLIP image scores for low-quality images. To address this issue, we suggest masking the objects in the source image that are truly relevant before computing the CLIP image score. We refer to this modified metric as Seg CLIP-I. As a result, we assess all the methods using three evaluation metrics: CLIP-I, Seg CLIP-I, and CLIP-T. (1) CLIP-I measures the average cosine similarity between the CLIP [21] embeddings of the generated images and the source images. (2) Seg CLIP-I is similar to CLIP-I, but all of the source images are processed with



**Table 2: Quantitative comparisons.** Our approach surpasses other methods in all aspects of multi-concept customization. Both our training and inference time rank among the fastest. The inference time metric is determined by 50-step sampling. The top-performing method’s metrics are shown in **red**, while the second-best method’s metrics are in **blue**.

Method	Single-Concept			Multi-concept			Training Time	Inference Time
	CLIP-I	Seg CLIP-I	CLIP-T	CLIP-I	Seg CLIP-I	CLIP-T		
TI [1]	0.738	0.721	0.752	0.666	0.660	0.736	23min	<b>7.50s</b>
DB [24]	<b>0.769</b>	0.736	0.775	0.637	0.652	<b>0.828</b>	10min	<b>7.35s</b>
Custom [8]	0.654	0.661	<b>0.813</b>	0.624	0.637	0.812	<b>4min</b>	7.53s
Cones2 [10]	0.768	<b>0.747</b>	0.758	<b>0.670</b>	<b>0.685</b>	0.816	26min	21.41s
Ours	<b>0.783</b>	<b>0.761</b>	<b>0.780</b>	<b>0.714</b>	<b>0.713</b>	<b>0.838</b>	<b>6min</b>	8.29s

	Source image	Source image(seg)	Good case	Bad case
CLIP-I with Source image	 1	 0.774	 0.772	 0.837
CLIP-I with Source image(seg)	0.774	1	0.739	0.735

**Fig. 6: CLIP-I v.s. Seg CLIP-I.** Our Seg CLIP-I more accurately reflects the fidelity differences between the “good case” and the “bad case” compared to CLIP-I.

segmentation on the relevant objects. (3) CLIP-T calculates the average cosine similarity between the prompt CLIP embeddings and image CLIP embeddings.

**Baselines.** We conduct comparisons between our method and four existing methods: Textual Inversion [1] (abbreviated as TI), DreamBooth [24] (abbreviated as DB), Custom Diffusion [8] (abbreviated as Custom), and Cones2 [10]. To ensure consistency, we implement Textual Inversion, DreamBooth, and Custom Diffusion using their respective Diffusers [19] versions. For Cones2, we implement it using its official code. All experimental settings follow the official recommended settings of each method.

## 4.2 Qualitative Comparison

We validate our method and all the comparison methods on various prompts. Specifically, these prompts include illustrating the relative positions of concepts, generating concepts in new situations, creating multi-concept images with a specific style, and associating different concepts with different prompts. In Fig. 5, the results of all comparative methods are generated by the base prompt which is presented under the images, while the results of our method are jointly generated through both the base prompt and region prompts. These generated images demonstrate that our method excels in generating high-quality multi-concept images while effectively adhering to different prompts.



**Fig. 7: Visualization of Ablation Studies.** We visualize the impact of removing specific components from our framework individually to demonstrate the importance of these methods.

### 4.3 Quantitative Comparison

As presented in Tab. 2, our method demonstrates superior image alignment compared to other methods in the single-concept setting. Additionally, our method achieves comparable text alignment, showcasing its adaptability to various complex prompts. In the multi-concept setting, our method outperforms all the compared methods in the three selected metrics, notably excelling in CLIP-I and Seg CLIP-I. Moreover, with excellent image fidelity and prompt alignment ability, our method does not incur significant training and inference costs. This indicates the effectiveness of our efficient concept encoding and regional customization module regarding multi-concept customization.

### 4.4 Ablation Study

**Without Regional Customization Module (Ours w/o region).** We conduct ablation experiments to validate the effectiveness of the regional customization module. In an attempt to directly load two LoRAs into the U-Net and generate images without utilizing the regional customization module, we find that this approach leads to feature confusion between different concepts and often only generates one object. As shown in Fig. 7, the features of the candle and teapot have fused to some extent under the prompt of “a  $S^*$  candle and a  $V^*$  teapot with a city in the background”, resulting in an output that contains both candle and teapot features. Moreover, such a generation method without the regional customization module produces only one object most of the time, which significantly lowers its CLIP-T in comparison to our approach as presented in Tab. 3.

**Table 3: Ablation Study.**

Method	CLIP-I	Seg CLIP-I	CLIP-T
Ours w/o Region	0.6918	0.7077	0.7104
Ours w/o QFormer	0.6911	0.6947	0.8238
Ours w/o ACN	0.6943	0.6951	0.8269
Ours	<b>0.7135</b>	<b>0.7126</b>	<b>0.8380</b>

**Without Training QFormer (Ours w/o QFormer).** In MiniGPT4 [35], the QFormer is completely frozen, and a linear layer is trained to project the output of the QFormer. Following this, we experiment by freezing the QFormer and training only a linear layer. As illustrated in Tab. 3, this approach results in

**Table 4: User Study.** The numbers represent the percentage (%) of users favoring the results of the methods. Our method is favored by the majority of users in the multi-concept setting for both text and image alignment.

	TI [1]		DB [24]		Custom [8]		Cones2 [10]		Ours	
	Text Alignment	Image Alignment	Text Alignment	Image Alignment	Text Alignment	Image Alignment	Text Alignment	Image Alignment	Text Alignment	Image Alignment
Single-Concept	37.72	39.20	45.22	58.08	<b>65.63</b>	22.48	45.58	47.94	63.01	<b>69.17</b>
Multi-Concept	21.13	34.02	38.00	23.96	35.50	18.64	44.93	38.04	<b>65.64</b>	<b>62.64</b>

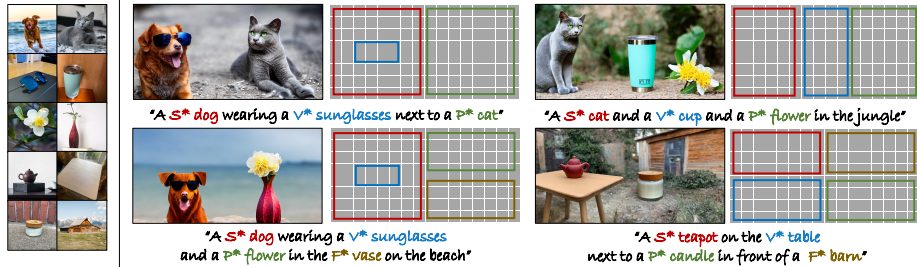


**Fig. 8: Challenge cases.** Our method consistently generates high-fidelity images when customizing a larger number of concepts.

a decrease in the learning capacity of concepts and consequently a decline in the representation capability of the generated customized embeddings. As a result, there is a noticeable decrease in all three selected metrics. Images generated by this approach also have lower fidelity compared to our method as shown in Fig. 7.

**Without adaptive concept normalization (Ours w/o ACN).** We conduct an ablation experiment to verify the effectiveness of the Adaptive Concept Normalization (ACN), which is used to mitigate the domain gap between the customized embedding and the other word embedding. As illustrated in Fig. 7 and Tab. 3, this domain gap leads to a decline in the customization ability, resulting in a notable decrease in image fidelity and prompt alignment ability compared to our method.

#### 4.5 User Study

We conduct user studies for all methods. For text alignment, we display an image of each method alongside its prompt and inquire, “Which images accurately represent the text description?”. For image alignment, we exhibit various training and generated images and ask, “Which images align best with the target images?”. Each questionnaire comprises 50 such inquiries. From a total of 460 received questionnaires, 72 are deemed invalid, resulting in 388 valid responses. As shown in Tab. 4, users prefer our approach for multi-concept generation regarding both text and image alignment.

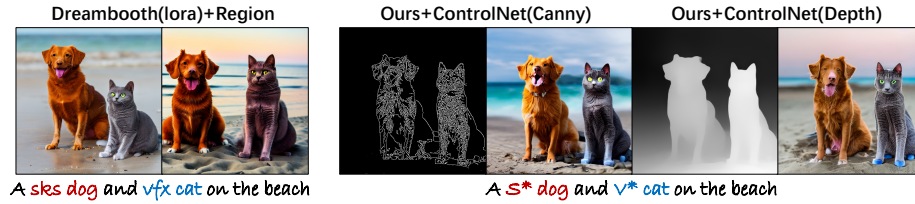


**Fig. 9: Extensions of our proposed MultiBooth.** Our methods can also be applied to LoRA-based DreamBooth and ControlNet.

#### 4.6 Challenge Cases

Our method theoretically enables the combination of an unlimited number of concepts, facilitating true multi-concept customization. In Fig. 8, we present the results of customizing three and four concepts, including a total of 10 concepts. The visualization demonstrates that our method consistently generates high-quality customization images when facing a larger number of concepts, further demonstrating the superiority of our approach.

#### 4.7 Extensions

**Enable DreamBooth to Perform Multi-concept Generation.** Our regional customization module can guide multiple LoRAs to conduct multi-concept generation, and it is adaptable to any LoRA-related method. An illustration of transferring the regional customization module to the LoRA-based DreamBooth [24] method has been provided. As shown in Fig. 9, with the support of the regional customization module, DreamBooth [24] is capable of the generation of multiple concepts. However, the absence of customized embeddings results in a decrease in fidelity.

**Apply ControlNet to our MultiBooth.** Our method is compatible with ControlNet [34] to achieve structure-controlled multi-concept generation. As illustrated in Fig. 9, our model inherits the architecture of the original U-Net model, resulting in satisfactory generations through seamless integration with pre-trained ControlNet without additional training.

## 5 Conclusion

In this paper, we introduce MultiBooth, a novel and efficient framework for multi-concept customization(MCC). Compared with existing MCC methods, our MultiBooth allows plug-and-play multi-concept generation with high image fidelity while bringing minimal cost during training and inference. By conducting qualitative and quantitative experiments, we robustly demonstrate our superiority over state-of-the-art methods within diverse multi-subject customization scenarios. Since current methods still require training to learn new concepts, in the future, we will investigate the task of training-free multi-concept customization based on our MultiBooth.

## References

- Gal, R., Alaluf, Y., Atzmon, Y., Patashnik, O., Bermano, A.H., Chechik, G., Cohen-Or, D.: An image is worth one word: Personalizing text-to-image generation using textual inversion. arXiv preprint arXiv:2208.01618 (2022) [2](#), [3](#), [4](#), [5](#), [7](#), [8](#), [11](#), [13](#)
- Gal, R., Arar, M., Atzmon, Y., Bermano, A.H., Chechik, G., Cohen-Or, D.: Encoder-based domain tuning for fast personalization of text-to-image models. *ACM Transactions on Graphics (TOG)* **42**(4), 1–13 (2023) [2](#), [4](#), [6](#)
- Goodfellow, I., Pouget-Abadie, J., Mirza, M., Xu, B., Warde-Farley, D., Ozair, S., Courville, A., Bengio, Y.: Generative adversarial networks. *Communications of the ACM* **63**(11), 139–144 (2020) [4](#)
- Gu, Y., Wang, X., Wu, J.Z., Shi, Y., Chen, Y., Fan, Z., Xiao, W., Zhao, R., Chang, S., Wu, W., et al.: Mix-of-show: Decentralized low-rank adaptation for multi-concept customization of diffusion models. arXiv preprint arXiv:2305.18292 (2023) [2](#)
- Hertz, A., Mokady, R., Tenenbaum, J., Aberman, K., Pritch, Y., Cohen-Or, D.: Prompt-to-prompt image editing with cross attention control. arXiv preprint arXiv:2208.01626 (2022) [2](#)
- Ho, J., Jain, A., Abbeel, P.: Denoising diffusion probabilistic models. *Advances in neural information processing systems* **33**, 6840–6851 (2020) [4](#)
- Hu, E.J., Shen, Y., Wallis, P., Allen-Zhu, Z., Li, Y., Wang, S., Wang, L., Chen, W.: Lora: Low-rank adaptation of large language models. arXiv preprint arXiv:2106.09685 (2021) [7](#)
- Kumari, N., Zhang, B., Zhang, R., Shechtman, E., Zhu, J.Y.: Multi-concept customization of text-to-image diffusion. In: *Proceedings of the IEEE/CVF Conference on Computer Vision and Pattern Recognition*. pp. 1931–1941 (2023) [2](#), [3](#), [4](#), [5](#), [7](#), [8](#), [10](#), [11](#), [13](#)
- Li, D., Li, J., Hoi, S.C.: Blip-diffusion: Pre-trained subject representation for controllable text-to-image generation and editing. arXiv preprint arXiv:2305.14720 (2023) [2](#), [6](#)
- Liu, Z., Zhang, Y., Shen, Y., Zheng, K., Zhu, K., Feng, R., Liu, Y., Zhao, D., Zhou, J., Cao, Y.: Cones 2: Customizable image synthesis with multiple subjects. arXiv preprint arXiv:2305.19327 (2023) [2](#), [3](#), [4](#), [5](#), [11](#), [13](#)
- Loshchilov, I., Hutter, F.: Decoupled weight decay regularization. arXiv preprint arXiv:1711.05101 (2017) [10](#)
- Lu, C., Zhou, Y., Bao, F., Chen, J., Li, C., Zhu, J.: Dpm-solver: A fast ode solver for diffusion probabilistic model sampling in around 10 steps. *Advances in Neural Information Processing Systems* **35**, 5775–5787 (2022) [10](#)
- Ma, Y., Cun, X., He, Y., Qi, C., Wang, X., Shan, Y., Li, X., Chen, Q.: Magic-stick: Controllable video editing via control handle transformations. arXiv preprint arXiv:2312.03047 (2023) [2](#)
- Ma, Y., He, Y., Cun, X., Wang, X., Shan, Y., Li, X., Chen, Q.: Follow your pose: Pose-guided text-to-video generation using pose-free videos. arXiv preprint arXiv:2304.01186 (2023) [2](#)
- Ma, Y., He, Y., Wang, H., Wang, A., Qi, C., Cai, C., Li, X., Li, Z., Shum, H.Y., Liu, W., et al.: Follow-your-click: Open-domain regional image animation via short prompts. arXiv preprint arXiv:2403.08268 (2024) [2](#)
- Ma, Y., Wang, Y., Wu, Y., Lyu, Z., Chen, S., Li, X., Qiao, Y.: Visual knowledge graph for human action reasoning in videos. In: *Proceedings of the 30th ACM International Conference on Multimedia*. pp. 4132–4141 (2022) [2](#)

17. Mou, C., Wang, X., Xie, L., Zhang, J., Qi, Z., Shan, Y., Qie, X.: T2i-adapter: Learning adapters to dig out more controllable ability for text-to-image diffusion models. arXiv preprint arXiv:2302.08453 (2023) [2](#)
18. Nichol, A., Dhariwal, P., Ramesh, A., Shyam, P., Mishkin, P., McGrew, B., Sutskever, I., Chen, M.: Glide: Towards photorealistic image generation and editing with text-guided diffusion models. arXiv preprint arXiv:2112.10741 (2021) [4](#)
19. von Platen, P., Patil, S., Lozhkov, A., Cuenca, P., Lambert, N., Rasul, K., Davaadorj, M., Wolf, T.: Diffusers: State-of-the-art diffusion models. <https://github.com/huggingface/diffusers> (2022) [11](#)
20. Qiao, T., Zhang, J., Xu, D., Tao, D.: Mirrorgan: Learning text-to-image generation by redescription. In: Proceedings of the IEEE/CVF Conference on Computer Vision and Pattern Recognition. pp. 1505–1514 (2019) [4](#)
21. Radford, A., Kim, J.W., Hallacy, C., Ramesh, A., Goh, G., Agarwal, S., Sastry, G., Askell, A., Mishkin, P., Clark, J., et al.: Learning transferable visual models from natural language supervision. In: International conference on machine learning. pp. 8748–8763. PMLR (2021) [4](#), [6](#), [8](#), [10](#)
22. Ramesh, A., Dhariwal, P., Nichol, A., Chu, C., Chen, M.: Hierarchical text-conditional image generation with clip latents. arXiv preprint arXiv:2204.06125 [1\(2\)](#), [3](#) (2022) [4](#)
23. Rombach, R., Blattmann, A., Lorenz, D., Esser, P., Ommer, B.: High-resolution image synthesis with latent diffusion models. In: Proceedings of the IEEE/CVF conference on computer vision and pattern recognition. pp. 10684–10695 (2022) [2](#), [4](#), [5](#), [9](#)
24. Ruiz, N., Li, Y., Jampani, V., Pritch, Y., Rubinstein, M., Aberman, K.: Dreambooth: Fine tuning text-to-image diffusion models for subject-driven generation. In: Proceedings of the IEEE/CVF Conference on Computer Vision and Pattern Recognition. pp. 22500–22510 (2023) [2](#), [3](#), [4](#), [5](#), [7](#), [8](#), [10](#), [11](#), [13](#), [14](#)
25. Saharia, C., Chan, W., Saxena, S., Li, L., Whang, J., Denton, E.L., Ghasemipour, K., Gontijo Lopes, R., Karagol Ayan, B., Salimans, T., et al.: Photorealistic text-to-image diffusion models with deep language understanding. Advances in Neural Information Processing Systems **35**, 36479–36494 (2022) [4](#)
26. Schuhmann, C., Beaumont, R., Vencu, R., Gordon, C., Wightman, R., Cherti, M., Coombes, T., Katta, A., Mullis, C., Wortsman, M., et al.: Laion-5b: An open large-scale dataset for training next generation image-text models. Advances in Neural Information Processing Systems **35**, 25278–25294 (2022) [4](#)
27. Shi, J., Xiong, W., Lin, Z., Jung, H.J.: Instantbooth: Personalized text-to-image generation without test-time finetuning. arXiv preprint arXiv:2304.03411 (2023) [4](#)
28. Wang, Q., Bai, X., Wang, H., Qin, Z., Chen, A.: Instantid: Zero-shot identity-preserving generation in seconds. arXiv preprint arXiv:2401.07519 (2024) [2](#)
29. Wei, Y., Zhang, Y., Ji, Z., Bai, J., Zhang, L., Zuo, W.: Elite: Encoding visual concepts into textual embeddings for customized text-to-image generation. arXiv preprint arXiv:2302.13848 (2023) [2](#), [4](#), [6](#)
30. Xu, T., Zhang, P., Huang, Q., Zhang, H., Gan, Z., Huang, X., He, X.: Attngan: Fine-grained text to image generation with attentional generative adversarial networks. In: Proceedings of the IEEE conference on computer vision and pattern recognition. pp. 1316–1324 (2018) [4](#)
31. Ye, H., Zhang, J., Liu, S., Han, X., Yang, W.: Ip-adapter: Text compatible image prompt adapter for text-to-image diffusion models. arXiv preprint arXiv:2308.06721 (2023) [2](#)



32. Zhang, H., Xu, T., Li, H., Zhang, S., Wang, X., Huang, X., Metaxas, D.N.: Stackgan: Text to photo-realistic image synthesis with stacked generative adversarial networks. In: Proceedings of the IEEE international conference on computer vision. pp. 5907–5915 (2017) [4](#)
33. Zhang, H., Xu, T., Li, H., Zhang, S., Wang, X., Huang, X., Metaxas, D.N.: Stackgan++: Realistic image synthesis with stacked generative adversarial networks. IEEE transactions on pattern analysis and machine intelligence **41**(8), 1947–1962 (2018) [4](#)
34. Zhang, L., Rao, A., Agrawala, M.: Adding conditional control to text-to-image diffusion models. In: Proceedings of the IEEE/CVF International Conference on Computer Vision. pp. 3836–3847 (2023) [2](#), [14](#)
35. Zhu, D., Chen, J., Shen, X., Li, X., Elhoseiny, M.: Minigtpt-4: Enhancing vision-language understanding with advanced large language models. arXiv preprint arXiv:2304.10592 (2023) [6](#), [12](#)